Quantum criticality and universality in the stationary state of the long-range Kitaev model

Akash Mitra [1,2] Sanku Paul,[3] and Shashi C. L. Srivastava [1,2]
[1] *Variable Energy Cyclotron Centre, 1/AF Bidhannagar, Kolkata 700064, India*
[2] *Homi Bhabha National Institute, Training School Complex, Anushaktinagar, Mumbai 400094, India*
[3] *Department of Physics and Complex Systems, S.N. Bose National Centre for Basic Sciences, Kolkata 700106, India*

(Received 15 November 2024; accepted 4 March 2025; published 12 March 2025)

We investigate the signature of quantum criticality in the long-time stationary state of the long-range Kitaev chain by performing various quench protocols. In this model, the pairing interaction decays with distance according to a power law with exponent α. Using quantum information-theoretic measures, such as mutual information and logarithmic negativity, we show that irrespective of the values of α, critical-to-critical quench displays quantum criticality even in the stationary state. Remarkably, in the presence of long-range pairing interactions, where fermionic correlators decay algebraically even at noncritical points, the signature of quantum criticality persists in the stationary state. Furthermore, the effective central charge, calculated from both mutual information and logarithmic negativity of the stationary state following a critical-to-critical quench, agrees with the central charge of the corresponding ground states for both $\alpha = 0$ and $\alpha = 2$. Therefore, information of the universality class can be inferred from the stationary state.

DOI: 10.1103/PhysRevB.111.104308

I. INTRODUCTION

Understanding quantum phase transitions (QPTs) has been a central topic of interest over the past few decades due to its significant implications for understanding the collective behavior of many-body systems [1]. QPTs have been both theoretically and experimentally studied extensively in various systems, including quantum spin chains [1–12], Bose-Einstein condensates [13–20], and strongly correlated electron systems [21–25]. QPT occurs at specific values of the parameter(s) present in the Hamiltonian, called critical points, where the system exhibits scale invariance. A universal behavior ensues due to the scale invariance, which can be classified into certain universality classes based on the space dimension and symmetry of the order parameter [26–29]. This universality is studied using conformal field theories and the corresponding central charge value is commonly used to identify the underlying universality class [30–32]. For instance, systems belonging to the Ising universality class are described by a minimal model with a central charge $c = 1/2$, while the Luttinger liquid universality class corresponds to a conformal bosonic theory with $c = 1$ [33,34]. Note that at quantum critical points, the development of long-range correlations leads to an algebraic decay of correlators over distance, in contrast to the exponential decay typically observed at noncritical points in Hamiltonians with only short-range interactions [35–38]. This is often used to identify critical points.

While the existence of quantum criticality and long-range correlations in the ground states of many-body quantum systems are widely studied, their presence in stationary states is not yet well explored. In Ref. [39], it is shown that when two sides of a one-dimensional (1D) noninteracting fermionic chain with nearest-neighbor hopping are prepared at different temperatures, the mutual information scales logarithmically with subsystem size in the steady state, indicating the presence of long-range correlations. Another example of the survival of quantum criticality in the long-time stationary state is shown in the anisotropic XY chain under a sudden quench protocol [40]. Using quantum information measures such as mutual information and logarithmic (log-) negativity, it is shown that when both the pre- and postquench parameters of the Hamiltonian are set at the critical point, both mutual information and log-negativity exhibit a peak, indicating the presence of criticality in the stationary state. In contrast, the peak in mutual information and log-negativity vanishes for other quench protocols when either/both pre- and postquench parameters differ from critical values. The signature of quantum criticality in the stationary state is attributed to a change in correlation pattern from exponential to algebraic decay, which was captured by mutual information and log-negativity.

A natural question follows: What about the scenario when correlators decay algebraically, even at noncritical points? Long-range interacting systems provide an ideal platform to explore this question as fermionic correlators have been shown to decay algebraically over distance, even when the Hamiltonian is gapped [41–44], i.e., at noncritical points. These long-range interacting systems have been studied in different contexts both theoretically and experimentally in atomic, molecular, and optical lattice systems [45–61]. We take the 1D long-range Kitaev model with a pairing term that decays with distance as a power law $\propto l^{-\alpha}$, with α being the exponent [44]. From an experimental perspective, this model is particularly relevant as it is closely related to the Ising model with tunable long-range interactions, which can be experimentally realized using trapped ion setups [53–55,57,58,62]. In the ground state, this model undergoes an exotic transition from the Ising-type universality class, observed for $\alpha > 3/2$, to a Luttinger liquid universality class at $\alpha = 0$.

In this paper, we investigate whether it is possible to capture quantum criticality in the stationary state when fermionic correlators decay algebraically even at noncritical points. Additionally, we examine whether the stationary state can be described by the same universality class as the ground state by analyzing the central charge obtained via scaling of mutual information and log-negativity for various quench protocols. Specifically, we consider three values of α corresponding to different universality classes observed in the ground state: first, corresponding to the Ising universality class ($\alpha = 2$); second, the Luttinger liquid universality class ($\alpha = 0$); and a third value ($\alpha = 1$) where there is no universality [44]. To understand the tripartite information in the postquench stationary state and whether signatures of criticality will manifest, we study tripartite mutual information.

II. THE MODEL AND GROUND-STATE PHASE TRANSITION

The Hamiltonian of the 1D long-range Kitaev model (LRK) for a lattice site of length N is expressed as [44]

$$H_{\rm LRK} = \sum_{j=1}^{N}\left[-t(f_j^\dagger f_{j+1} + f_{j+1}^\dagger f_j) - \mu\left(f_j^\dagger f_j - \frac{1}{2}\right) + \frac{\Delta}{2}\sum_{l=1}^{N-1}\frac{1}{l^\alpha}(f_{j+l}^\dagger f_j^\dagger - f_{j+l}f_j)\right], \quad (1)$$

where $f_j(f_j^\dagger)$ is the fermionic annihilation (creation) operator at site j, satisfying the canonical anticommutation relations $\{f_i, f_j^\dagger\} = \delta_{ij}$, $\{f_i, f_j\} = \{f_i^\dagger, f_j^\dagger\} = 0$. The parameters t and μ represent the tunneling rate between two neighboring sites and the chemical potential, respectively. We set $2t = 1$ in the rest of the paper. The parameter Δ denotes the strength of the fermion p-wave pairing interaction, while its range is governed by the exponent $\alpha \in [0, \infty)$. The two limits, i.e., $\alpha = 0$ and $\alpha \to \infty$, correspond to all-to-all interaction with equal strength and nearest-neighbor interaction, respectively. We consider the antiperiodic boundary condition throughout the paper. The Hamiltonian in Eq. (1) is exactly solvable. To see this, we first perform a Fourier transformation to transform Eq. (1) in the momentum space as

$$H_{\rm LRK} = \frac{1}{2}\sum_{n=0}^{N-1}[f_{k_n}^\dagger \quad f_{N-k_n}] \times \begin{bmatrix} -(\mu + \cos k_n) & i\Delta g_\alpha(k_n) \\ -i\Delta g_\alpha(k_n) & (\mu + \cos k_n) \end{bmatrix}\begin{bmatrix} f_{k_n} \\ f_{N-k_n}^\dagger \end{bmatrix}, \quad (2)$$

where $g_\alpha(k) = \sum_{l=1}^{N-1}\frac{\sin(kl)}{l^\alpha}$ and $k_n = \frac{2\pi}{N}(n + 1/2)$. In the large-$N$ limit, $g_\alpha(k)$ takes the form

$$g_\alpha(k) = -\frac{i}{2}[{\rm Li}_\alpha(e^{ik}) - {\rm Li}_\alpha(e^{-ik})]. \quad (3)$$

The function ${\rm Li}_\alpha(z)$ represents the polylogarithm of the complex variable z of order α. The Hamiltonian in Eq. (2) can further be cast to a diagonal form by performing the following Bogoliubov transformation:

$$\begin{bmatrix} f_{k_n} \\ f_{N-k_n}^\dagger \end{bmatrix} = \begin{bmatrix} \cos\theta_{k_n} & -i\sin\theta_{k_n} \\ -i\sin\theta_{k_n} & \cos\theta_{k_n} \end{bmatrix}\begin{bmatrix} \eta_{k_n} \\ \eta_{N-k_n}^\dagger \end{bmatrix}, \quad (4)$$

TABLE I. Summary of the effective central charge $c_{\rm eff}$ for different values of α and μ for the ground state of the long-range Kitaev model [42,44,63,64].

	$\alpha = 0$	$0 < \alpha \leqslant 1$	$\alpha \to \infty$
$\mu = 1$	1	$c_{\rm eff}(\alpha, \Delta) \neq 0$	$\frac{1}{2}$
$\mu \neq \pm 1$	$\frac{1}{2}$	$c_{\rm eff}(\alpha, \Delta) \neq 0$	0

with θ being the Bogoliubov angle, and defined as

$$\tan\left(2\theta_{k_n}\right) = \frac{\Delta g_\alpha(k_n)}{\mu + \cos k_n}. \quad (5)$$

The diagonal form of the Hamiltonian in Eq. (1) in the basis of Bogoliubov fermions η then becomes

$$H_{\rm LRK} = \sum_{n=0}^{N-1}\lambda_\alpha(k_n)\left(\eta_{k_n}^\dagger\eta_{k_n} - \frac{1}{2}\right), \quad (6)$$

where the dispersion relation is

$$\lambda_\alpha(k_n) = \sqrt{(\mu + \cos k_n)^2 + [\Delta g_\alpha(k_n)]^2}. \quad (7)$$

Equation (6) signifies that each mode is independent, implying the integrability of the system. In the limit $\alpha \to \infty$, only nearest-neighbor terms contribute to the sum in $g_\alpha(k)$, resulting in $g_\infty(k) = \sin(k)$. The Hamiltonian in Eq. (1) in this limit coincides with the Hamiltonian of the XY model obtained via the Jordan-Wigner transformation. For the XY model, a ground-state phase transition occurs from the gapped ferromagnetic ordered phase to the gapped paramagnetic disordered phase with increasing the chemical potential $|\mu|$, with the two critical gapless points at $\mu = \pm 1$ [44]. The spectrum in Eq. (7) continues to be gapless at $\mu = \pm 1$, even with the smaller values of α, i.e., in the presence of long-range interactions as long as $\alpha > 1$. However, the phase diagram changes for $\alpha < 1$. This regime is referred to as "strong" long-range regime since $\alpha < d$, with d representing the dimension of the system. In comparison to $\alpha > 1$, one significant change is that $\mu = -1$ is no longer a critical point, and the phase diagram is no longer symmetric across the line $\mu = 0$ [42,44]. A good probe to identify these critical points is the von Neumann entropy S_{vN}, expressed as $S_{vN} = -{\rm Tr}(\rho_L \ln \rho_L)$, where ρ_L is the reduced density matrix of the subsystem of length L. At these critical points, where the spectral gap closes, S_{vN} for short-range interacting system scales as [65–68]

$$S_{vN} \approx \frac{c}{3}\ln\left[\frac{N}{\pi}\sin\left(\frac{\pi L}{N}\right)\right] + c', \quad (8)$$

where c is the central charge of the underlying conformal field theory (CFT), N is the total system size, and c' is a nonuniversal constant. In fact, Eq. (8) is also valid for all values of α and μ, but the central charge c is now replaced with an effective central charge $c_{\rm eff}$ [44,63]. The values of the $c_{\rm eff}$ for the ground state are summarized in Table I. It is worth mentioning that $\alpha = 0$ signifies all-to-all coupling between the sites and falls under the Tomonaga-Luttinger liquid universality class [69].

III. METHODS

In the last section, we summarized criticality seen in the ground state of the LRK model and (effective) central charge of the underlying CFT. A natural question then arises: Does this criticality survive when the system undergoes out-of-equilibrium dynamics? In other words, in a stationary state, can we find any signature of quantum criticality? A common way to achieve the nonequilibrium dynamics is through sudden quench where the local or global parameters of the system are suddenly changed [70]. As a consequence, the ground state of the prequench Hamiltonian is no longer a ground state of the postquench Hamiltonian, but a superposition of its eigenstates. The long-time stationary state of the LRK model under sudden quench is the system of interest. To probe the criticality, much like the ground state, entanglement entropy would be our first choice. However, as the long-time stationary state typically involves highly excited states, S_{vN} exhibits volume-law scaling eclipsing the logarithmic dependence on subsystem size which may be present due to criticality. So, to extract these logarithmic correlations, we consider quantum information-theoretic measures such as mutual information and log-negativity. For the ground state, mutual information has already been established to capture the criticality in fermionic systems [71].

Mutual information. The mutual information between two subsystems A_1 and A_2 is defined as

$$I_{A_1:A_2} = S_{vN}^{A_1} + S_{vN}^{A_2} - S_{vN}^{A_1\cup A_2}, \tag{9}$$

where $S_{vN}^{A_1}(S_{vN}^{A_2})$ is the von Neumann entropy of the subsystem $A_1(A_2)$ and $S_{vN}^{A_1\cup A_2}$ is the von Neumann entropy of $A_1 \cup A_2$. Throughout the paper, we consider the subsystem sizes $|A_1| = |A_2| = L$. The mutual information between two subsystems measures the total amount of information (both classical and quantum) that one subsystem contains about the other [72]. Furthermore, if S_{vN} of the long-time stationary state contains both the volume and logarithmic terms, the mutual information should scale as $I_{A_1:A_2} \sim b \ln L$. Thus, if the long-range correlations are present in the stationary state, then the mutual information should behave as [39,40,73–76]

$$I_{A_1:A_2} \sim \frac{c_{\text{eff}}^I}{3} \ln L + \text{const}, \tag{10}$$

where we define c_{eff}^I as the effective central charge of the stationary state extracted using mutual information. In this way, mutual information can capture the logarithmic correlation that is hidden in S_{vN}. However, whether these correlations are truly quantum in nature remains to be investigated. In this context, log-negativity serves as a useful measure.

Log-negativity. Similar to mutual information, log-negativity, an entanglement monotone, also quantifies the nonlocal correlation between two subsystems. But unlike mutual information, it captures only quantum correlations [77–80]. It is defined as [77,78]

$$\xi_{A_1:A_2} \equiv \ln \left|\left|\rho_A^{T_2}\right|\right| = \ln \text{Tr}\left|\rho_A^{T_2}\right|, \tag{11}$$

where $||\cdot||$ denotes the trace norm, and $\rho_A^{T_2}$ signifies the partial transposition of the reduced density matrix of $A \equiv (A_1 \cup A_2)$. It is worth mentioning that for a CFT, the expression of log-negativity for two adjacent subsystems each of length L_1 and L_2, respectively, is shown to be [81]

$$\xi_{A_1:A_2} = \frac{c}{4} \ln \left(\frac{L_1 L_2}{L_1 + L_2}\right), \tag{12}$$

where c is the central charge. For the XY model, during a critical-to-critical quench, the log-negativity of the long-time stationary state scales as $\xi_{A_1:A_2} = \frac{1}{8} \ln L$, where $L_1 = L_2 = L$ [40]. The logarithmic divergence of $\xi_{A_1:A_2}$ is consistent with the critical ground state, as the XY model belongs to the Ising universality class with $c = 1/2$. Based on this, we assume that if there is any signature of long-range quantum correlations in the long-time stationary state, the log-negativity would exhibit the following scaling behavior:

$$\xi_{A_1:A_2} \sim \frac{c_{\text{eff}}^N}{4} \ln L + \text{const}, \tag{13}$$

where c_{eff}^N represents the effective central charge of the stationary state extracted using the log-negativity.

Time evolution. For noninteracting free-fermionic chains, owing to the simple relationship between the eigenvalues of the reduced density matrix and two-point correlation function, we can calculate the entanglement entropy more efficiently by defining correlation matrix W as

$$W_{nm} = \text{Tr}\left(\rho \begin{bmatrix} f_n \\ f_n^\dagger \end{bmatrix} [f_m^\dagger \quad f_m]\right) = \begin{bmatrix} \delta_{nm} - C_{nm} & F_{nm} \\ \overline{F_{nm}} & C_{nm} \end{bmatrix}, \tag{14}$$

where $n, m = 1, \dots, L$. The functions C_{nm} and F_{nm} are two-point correlation functions, defined as $C_{nm} = \langle f_n^\dagger f_m \rangle$ and $F_{nm} = \langle f_n f_m \rangle$. The expectation value $\langle\cdot\rangle$ is taken with respect to the state of interest and the overbar represents complex conjugation. The correlation matrix W is a Hermitian matrix with eigenvalues lying on the real interval [0,1]. Given the correlation matrix, S_{vN} can be evaluated as [64,66,82]

$$S = -\tfrac{1}{2}\text{Tr}[(I - W)\ln(I - W) + W \ln W]. \tag{15}$$

At any finite time t, the correlation functions are given by $C_{nm}(t) = \langle f_n^\dagger(t) f_m(t)\rangle$ and $F_{nm}(t) = \langle f_n(t) f_m(t)\rangle$, where the expectation values are taken with respect to the time-evolved state obtained under the operation of the postquench Hamiltonian. The two time-dependent correlation functions, $C_{nm}(t)$ and $F_{nm}(t)$, are expressed as [83]

$$\begin{aligned}\langle f_j(t) f_{j+l}(t)\rangle = \frac{1}{2N}\sum_{n=0}^{N-1} e^{ik_n l}\Big(&-\sin\left[2\lambda_\alpha^f(k_n)t\right]\sin\left(2\delta\theta_{k_n}\right)\\ &+ i\left\{\sin\left(2\theta_{k_n}\right)\cos\left(2\delta\theta_{k_n}\right)\right.\\ &\left.-\cos\left[2\lambda_\alpha^f(k_n)t\right]\sin\left(2\delta\theta_{k_n}\right)\cos\left(2\theta_{k_n}\right)\right\}\Big),\\ \langle f_j^\dagger(t) f_{j+l}(t)\rangle = \frac{1}{2N}\sum_{n=0}^{N-1} e^{-ik_n l}\Big\{&1 - \cos\left(2\theta_{k_n}\right)\cos\left(2\delta\theta_{k_n}\right)\\ &-\sin\left(2\theta_{k_n}\right)\sin\left(2\delta\theta_{k_n}\right)\cos\left[2\lambda_\alpha^f(k_n)t\right]\Big\},\end{aligned} \tag{16}$$

where $\delta\theta_{k_n} = \theta_{k_n}^f - \theta_{k_n}^i$ is the difference between pre- and postquench Bogoliubov angles defined in Eq. (5) and $\lambda_\alpha^f(k_n)$ is defined by Eq. (7) for the postquench Hamiltonian.

In the limit $t \to \infty$, the time-dependent sine and cosine functions become highly oscillatory and the respective sum would tend to zero. Using this approximation, the expression for the correlation functions in the long-time stationary state is given by

$$\langle f_j f_{j+l}\rangle_{\rm st} = \frac{i}{2N}\sum_{n=0}^{N-1} e^{ik_n l}\sin\left(2\theta_{k_n}\right)\cos\left(2\delta\theta_{k_n}\right),$$

$$\langle f_j^\dagger f_{j+l}\rangle_{\rm st} = \frac{1}{2N}\sum_{n=0}^{N-1} e^{ik_n l}\left[1-\cos\left(2\theta_{k_n}\right)\cos\left(2\delta\theta_{k_n}\right)\right], \quad (17)$$

where $\langle f_j^\dagger f_{j+l}\rangle_{\rm st}$ and $\langle f_j f_{j+l}\rangle_{\rm st}$ are the two-point correlation and two-point anomalous correlation functions for the stationary state. We utilize the above two expressions to generate the correlation matrix W, as defined by Eq. (14), and then apply Eq. (15) and Eq. (9) to obtain S_{vN} and $I_{A_1:A_2}$, respectively, for the long-time stationary state.

Numerical estimation of log-negativity. Equation (11) suggests that to evaluate log-negativity, the crucial part is to perform the partial transposition. Unfortunately, the partial transposition of a fermionic Gaussian state is not a Gaussian state [84,85]. This makes it difficult to efficiently calculate log-negativity in noninteracting fermionic systems. However, by expressing the partial transposition as a linear combination of two Gaussian operators, an upper bound on log-negativity can be obtained and is expressed as [40,84–89]

$$\xi^u_{A_1:A_2} = \ln {\rm Tr}(O_+O_-)^{\frac{1}{2}} + \ln\sqrt{2}, \quad (18)$$

where the trace norm of O_+ is given by

$$||O_+|| = {\rm Tr}(O_+O_-)^{\frac{1}{2}} = \det\left[\left(\frac{\mathbb{1}+i\Gamma_x}{2}\right)^{\frac{1}{2}} + \left(\frac{\mathbb{1}-i\Gamma_x}{2}\right)^{\frac{1}{2}}\right] \times \det\left(\frac{\mathbb{1}-\tilde{\Gamma}_1\tilde{\Gamma}_2}{2}\right), \quad (19)$$

with

$$\Gamma_x = i[1-(1+i\tilde{\Gamma}_2)(1-\tilde{\Gamma}_1\tilde{\Gamma}_2)^{-1}(1+i\tilde{\Gamma}_1)]. \quad (20)$$

The quantities $\tilde{\Gamma}_1$, $\tilde{\Gamma}_2$ in Eqs. (19) and (20) are defined as

$$\tilde{\Gamma}_k = \tilde{M}_2\Gamma_k\tilde{M}_2\,, \quad M_2 = \begin{bmatrix} \mathbb{1}_L & 0 \\ 0 & i\,\mathbb{1}_L\end{bmatrix}, \quad (21)$$

and the size of the subsystems $|A_1| = |A_2| = L$. The correlation matrices Γ_1 and Γ_2 are defined as

$$\Gamma_1 = \Gamma^A, \quad \Gamma_2 = M_2\Gamma_1M_2, \quad M_2 = \begin{bmatrix} \mathbb{1}_L & 0 \\ 0 & -\mathbb{1}_L\end{bmatrix}, \quad (22)$$

where Γ^A is the correlation matrix corresponding to the subsystem A ($A = A_1 \cup A_2$) and is defined as $\Gamma^A = 2W - I$. With Eqs. (19), (21), and (22), the upper bound of log-negativity can be evaluated using Eq. (18).

IV. RESULTS

A. Signature of criticality in stationary state

As we look for the signature of quantum criticality in the long-time stationary state for different α values, we consider two types of quench protocols which differ in the initial states. In the first protocol, we consider the initial state as the ground state of the LRK Hamiltonian corresponding to the parameter values $\mu_i = 1$ and $\Delta_i = -1$ and is henceforth referred to as the critical state. The second protocol corresponds to the initial state as the ground state of the LRK Hamiltonian corresponding to parameters $\mu_i = 1.5$ and $\Delta_i = -1$, which is henceforth referred to as the noncritical state. The final Hamiltonian parameters, μ_f and Δ_f, are varied to include both the critical and noncritical regimes. Note that it has already been established that mutual information of the ground state shows a peak at the critical point, namely, $\mu = \pm 1$ for large $\alpha (= 10)$, while only at $\mu = 1$ for $\alpha \leqslant 1$ [71]. Mutual information $I_{A_1:A_2}$ calculated for the stationary state for both quench protocols, i.e., $(\mu_i = 1, \Delta_i = -1) \to (\mu_f = \mu, \Delta_f = 1)$ and $(\mu_i = 1.5, \Delta_i = -1) \to (\mu_f = \mu, \Delta_f = 1)$, is plotted in Fig. 1 (row 1). For the final quench parameters corresponding to critical values, a peak in $I_{A_1:A_2}$ for the critical initial state is clearly visible, indicating the signature of the criticality in the stationary state for all values of α. In the other quench protocol with the noncritical initial state, $I_{A_1:A_2}$

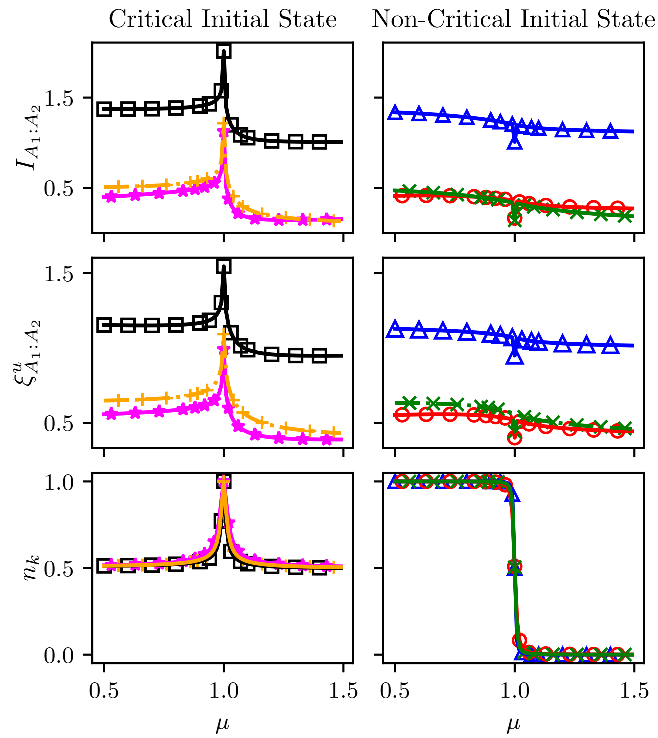

FIG. 1. Top row: The mutual information between two subsystems, $I_{A_1:A_2}$, of the stationary state as a function of the postquench chemical potential $\mu_f = \mu$, for three values of α: $\alpha = 0$ (black squares), $\alpha = 1$ (magenta stars), and $\alpha = 2$ (orange pluses). The prequench chemical potential μ_i is set at the critical point (left column), i.e., $\mu_i = 1$, and at a noncritical point (right column), i.e., $\mu_i = 1.5$. For noncritical initial state (right column), blue triangles correspond to $\alpha = 0$, red circles to $\alpha = 1$ and green crosses to $\alpha = 2$. Middle row: The log-negativity of the stationary state using the same symbols and quench parameters as the top row. Bottom row: The occupation probability n_k of Bogoliubov fermions at the soft mode, calculated from Eq. (23), with the same symbols and quench parameters as in the top row. For all figures, the quench protocol for the strength of the p-wave pairing interaction Δ is chosen as $\Delta_i = -1$ and $\Delta_f = 1$.

does show a nonanalytic behavior in the form of a sharp dip for $\mu_f = 1$ for all values of α. To confirm that this behavior is indeed due to the quantum nature of correlations, we plot log-negativity $\xi_{A_1:A_2}$ in Eq. (11) in Fig. 1 (row 2) for the same quench protocols. The similar peak and dip structure is unmistakably seen in the behavior of $\xi_{A_1:A_2}$ whenever the final Hamiltonian is critical. Such behavior of $I_{A_1:A_2}$ for the nearest-neighbor free-fermionic model has earlier been explained in terms of a soft mode for which the energy vanishes near criticality. For a critical-to-critical quench, the soft mode does not get excited, resulting in a peak structure in $I_{A_1:A_2}$ while it heats up to infinite temperature for a noncritical-to-critical quench displaying a dip in $I_{A_1:A_2}$. This further manifests as an algebraic decay of fermionic correlation for critical-to-critical quench, akin to ground-state behavior, while for the noncritical-to-critical quench, it decays exponentially, indicating a noncritical behavior. However, such an explanation falls short for the LRK model for $\alpha \leqslant 1$, as the correlation decay pattern in the ground state is always algebraic.

For this nonanalytic behavior of entanglement measure at $\mu_f = 1$, we offer an alternate explanation in terms of the mode occupation probability n_k for the soft mode ($k_c = \pi$) where the energy vanishes near criticality. Let us recall that $n_{k_c} = 1/2$ would imply a contribution from multiple modes and therefore leads to higher entanglement entropy for the union of two subsystems, $S_{vN}^{A_1 \cup A_2}$. As in $I_{A_1:A_2}$ in Eq. (9), $S_{vN}^{A_1 \cup A_2}$ is being subtracted; this leads to a decrease in $I_{A_1:A_2}$. In contrast, $n_{k_c} = 1, 0$ will lead to a reduction of $S_{vN}^{A_1 \cup A_2}$ and, consequently, leads to an increment of the mutual information.

The occupation probability, $n_k = \langle \eta_k^\dagger \eta_k \rangle$ of the Bogoliubov modes, η_k, in the stationary state of the LRK model is obtained as

$$\langle \eta_k^\dagger \eta_k \rangle = \frac{1}{2}[1 - \cos(2\delta\theta_k)] = \frac{1}{2}\left[1 - \frac{(\mu_f + \cos k)(\mu_i + \cos k) + \Delta_f \Delta_i g_\alpha^2(k)}{\lambda_\alpha^f(k)\lambda_\alpha^i(k)}\right], \tag{23}$$

where $\lambda_\alpha^i(k)$ ($\lambda_\alpha^f(k)$) denotes the energy corresponding to the prequench (postquench) Hamiltonian. From Eq. (23), it can be shown that if we start with the noncritical initial state, i.e., $\mu_i = 1.5$, in the limit $k \to \pi$, the occupation probability n_k is given by

$$n_k = \begin{cases} 1 & \text{for } \mu < 1, \\ \frac{1}{2} & \text{for } \mu = 1, \\ 0 & \text{for } \mu > 1, \end{cases} \tag{24}$$

as illustrated in Fig. 1 (row 3). This explains the dips observed in I_{A_1,A_2} in the long-time stationary state for a noncritical-to-critical quench. In contrast, for the quench protocol involving the critical state, n_k near the soft mode is

$$n_k = \begin{cases} \frac{1}{2} & \text{for } \mu < 1, \\ 1 & \text{for } \mu = 1, \\ \frac{1}{2} & \text{for } \mu > 1. \end{cases} \tag{25}$$

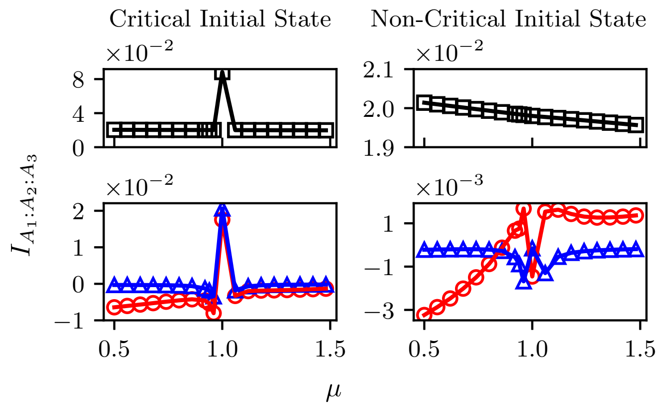

FIG. 2. We plot the tripartite mutual information for different values of postquench μ by fixing the prequench μ_i at $\mu_i = 1$ (left column) and $\mu_i = 1.5$ (right column) for $\alpha = 0$ (black squares), $\alpha = 1$ (red circles), and $\alpha = 2$ (blue triangles). The quench protocol for Δ is chosen to be the same as in Fig. 1.

This explains the peak observed in $I_{A_1:A_2}$ for the critical-to-critical quench protocol.

Going beyond the search for signatures of criticality in the bipartite information-theoretic measures such as mutual information and log-negativity, we now study the tripartite mutual information whose negative, zero, and positive values indicate perfectly delocalized or scrambled information, extensivity of mutual information, and redundancy of information [90–92]. For the completeness, the tripartite mutual information (TMI) is defined as

$$I_{A_1:A_2:A_3} = I_{A_1:A_2} + I_{A_1:A_3} - I_{A_1:A_2 \cup A_3}, \tag{26}$$

where $I_{A_i:A_j}$ is the mutual information between A_i and A_j [93]. It is known that for 1D noncritical systems, $I_{A_1:A_2:A_3}$ approaches zero in the large system limit [94]. For the same quench protocols used in the study of mutual information, TMI for the stationary state is presented in Fig. 2. Similar to the bipartite mutual information, the TMI for the stationary state obtained post critical-to-critical quench also exhibits a peak at $\mu = 1$. In contrast, a nonanalytical behavior of TMI for the stationary state is visible for noncritical-to-critical quench. This indicates that the criticality associated with the stationary state can also be captured through tripartite mutual information, which is a measure of nonlocal correlations. Moreover, a negative TMI for $\mu < 1$ shows the presence of nonlocal information, but a redundancy of information for $\mu > 1$ for $\alpha = 1$. The short-range pairing term, i.e., $\alpha = 2$, displays zero TMI everywhere except at the critical point, in agreement with the existing literature. An all-to-all pairing term, however, has an entirely different behavior where TMI is always positive, suggesting a redundancy of information, which peaks at the critical point, $\mu = 1$.

B. Signature of universality in stationary state

After establishing the nonanalytic behavior of mutual information (and log-negativity) for the postquench stationary state at the critical point of the postquench Hamiltonian, a

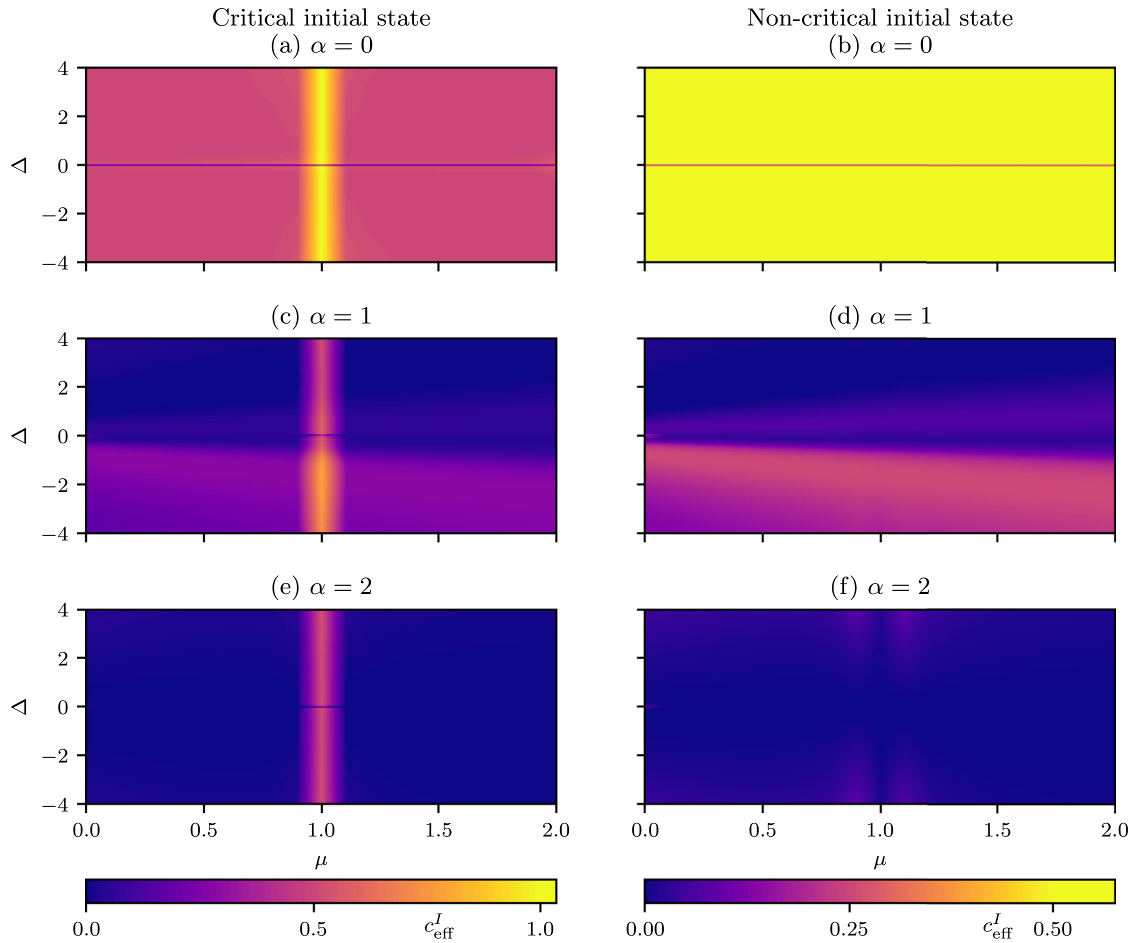

FIG. 3. Phase plot of effective central charge $c^I_{\rm eff}$ extracted from mutual information in the postquench $\Delta - \mu$ plane for both critical (left column) and noncritical (right column) initial state for $\alpha = 0$ (top row), 1 (middle row) and 2 (bottom row). The parameter Δ_i is fixed at -1 for all the plots.

natural question arises: Does the information of the effective central charge, $c^I_{\rm eff}$ ($c^N_{\rm eff}$), calculated from the scaling of $I_{A_1:A_2}$ ($\xi_{A_1:A_2}$), depend on the quench protocol? And is this effective central charge universal, i.e., independent of quench protocols in Δ; if yes, is the central charge of the ground state conserved? To address these questions, we analyze both $c^I_{\rm eff}$ and $c^N_{\rm eff}$ for both of the quench protocols discussed in Sec. IV A. Here, it is useful to recall that central charge provides a powerful tool to understand the underlying CFT that describes the particular universality class [33]. For instance, the Ising universality class and the Luttinger liquid universality class are described by a completely different CFT and characterized by distinct central charges. The central charge gives a measure of the number of degrees of freedom or the "size" of the symmetry in the theory [95,96].

Figure 3 displays $c^I_{\rm eff}$ as a function of the postquench parameters μ_f and Δ_f. The columns of Fig. 3 represent $c^I_{\rm eff}$ for quenches starting with two distinct initial states, while the rows correspond to a varying range of α. Let us focus on the left column, i.e., the quench from the critical state for different values of α. For both $\alpha = 0$ and $\alpha = 2$, $c^I_{\rm eff}$ is independent of Δ quenches and retains the same value as the ground state for a critical-to-critical quench protocol. For other values of μ_f, $c^I_{\rm eff}$ calculated from the stationary state takes the value of the noncritical ground state, i.e., 0.5 for $\alpha = 0$ and 0 for $\alpha = 2$ [97]. For $\alpha = 1$, the effective central charge for the ground state at the critical point depends on the value of Δ and this character is retained in the postquench stationary state as well. Therefore, the universality can only be discussed in the cases of $\alpha = 0$ and $\alpha = 2$ from a critical-to-critical quench. It is clearly seen that $c^I_{\rm eff}$ calculated from the postquench stationary state conserves the central charge (see Table I). This implies that the universality class for the critical ground state can also be inferred from the stationary state.

Now for the right column of Fig. 3, the universal characteristic of the $c^I_{\rm eff}$ of the stationary state is reflected through the independence of Δ quenches for $\alpha = 0$ and $\alpha = 2$, while $\alpha = 1$ remains Δ dependent. Note that even though the entanglement measures showed a nonanalytic behavior at $\mu_f = 1$ for the noncritical initial state, the effective central charge does not show any such transition for either $\alpha = 0$ or 2. Therefore, despite the nonanalytic behavior of entanglement measures at $\mu_f = 1$, we do not attribute it as a signature of criticality or a universal description in terms of the underlying CFT.

TABLE II. Summary of effective central charge values calculated from the postquench stationary state for critical-to-critical, noncritical-to-critical, and critical-to-noncritical quenches of the LRK model for different values of α.

	$\alpha = 0$	$0 < \alpha \leqslant 1$	$\alpha = 2$
$\mu_i = 1, \mu_f = 1$	1	$c_{\text{eff}}(\alpha, \Delta) \neq 0$	$\frac{1}{2}$
$\mu_i \neq 1, \mu_f = 1$	$\frac{1}{2}$	$c_{\text{eff}}(\alpha, \Delta) \neq 0$	0
$\mu_i = 1, \mu_f \neq 1$	$\frac{1}{2}$	$c_{\text{eff}}(\alpha, \Delta) \neq 0$	0

Therefore, to summarize, the signature of universality in terms of effective central charge is seen in the postquench stationary state for a critical-to-critical quench. The effective central charges values in this case are summarized in tabular form in Table II, and are in agreement with the values in Table I calculated for the ground state.

Now, to investigate whether the long-range correlations in the stationary state are genuinely quantum in nature, we have evaluated the effective central charge c^N_{eff} extracted from the finite-size scaling of the log-negativity for the stationary state. While the details are in Appendix A, the findings of the effective central charge behavior and therefore universality remain the same as those calculated using mutual information.

V. SUMMARY

In summary, we studied the quench dynamics of the long-range Kitaev chain to investigate the possible signatures of quantum criticality in the long-time stationary state for different values of the exponent α characterizing the range of p-wave pairing interaction. To probe the criticality, we consider the quantum information-based measures such as bipartite and tripartite mutual information, and log-negativity. Our results show that a peak emerges at $\mu = 1$ in bipartite mutual information, tripartite mutual information, and log-negativity for a critical-to-critical quench for all values of α studied in this work, exhibiting behavior similar to that of the critical ground state. This clearly indicates the presence of criticality in the stationary state. Importantly, in contrast to the short-range XY model, the appearance of this peak cannot be attributed to the change in decay pattern of the fermionic correlation from exponential to algebraic at the critical point, as the fermionic correlators decay algebraically even at noncritical points for $\alpha \leqslant 1$. We argue that the peak in bipartite mutual information arises due to the change in the occupation probability of the Bogoliubov fermions in the soft mode at the critical point. To understand the longer-range quantum information in a postquench stationary state, we studied the TMI, which not only captures the signature of criticality but also shows that quantum correlations are delocalized for the $\mu < 1$ case and have redundancy for $\mu > 1$ for $\alpha = 1$. For pairing exponent $\alpha = 2$, the mutual information is extensive for all values of μ except $\mu = 1$, while for $\alpha = 0$, the quantum correlations show redundancy.

We further show that for $\alpha = 2$, long-range correlations develop only for the critical-to-critical quench. This result is obtained by analyzing the effective central charges extracted from bipartite mutual information and log-negativity scaling analysis. The effective central charge of the corresponding stationary state matches the same for the critical ground state, regardless of the quench in the strength of the p-wave pairing interaction, Δ. This match indicates that the universality class for the critical ground state can also be inferred from the stationary state. In contrast, for $\alpha = 0$, the effective central charge is nonzero for all quench protocols, leading to long-range correlations, except when the final Hamiltonian parameter $\Delta = 0$. When $\Delta \neq 0$, the effective central charge is 1 only for the critical-to-critical quench and is $1/2$ for all other quench protocols, consistent with the ground state. This consistency suggests that the stationary state for the critical-to-critical quench protocol belongs to the same universality class as the ground state.

For $\alpha = 1$, the stationary state, similar to the ground state, cannot be described by any universality class, as the presence or absence of long-range correlations depends on the Δ quenches. However, long-range correlations develop for the critical-to-critical quench protocol, regardless of the Δ quenches.

ACKNOWLEDGMENT

S.P. would like to thank DST India for the Inspire Faculty Grant.

APPENDIX: OVERVIEW OF CENTRAL CHARGE FOR POSTQUENCH STATIONARY STATE FROM LOG-NEGATIVITY

Starting with the critical initial state, as shown in the top row, left column of Fig. 4, we find that for $\alpha = 0$, $c^N_{\text{eff}} = 1/2$ for $\mu_f \neq 1$ and $\Delta_f \neq 0$, while $c^N_{\text{eff}} = 1$ for $\mu_f = 1$ and $\Delta_f \neq 0$. In contrast, starting with a noncritical initial state, as shown in the top row, right column of Fig. 4, $c^N_{\text{eff}} = 1/2$ for all values of μ_f and Δ_f, except for $\Delta_f = 0$. This implies that for $\alpha = 0$, $c^N_{\text{eff}} = c^I_{\text{eff}}$ for all quench protocols. For $\alpha = 2$, similar to c^I_{eff}, c^N_{eff} is nonzero and equal to $1/2$ only for a critical-to-critical quench protocol (with the exception of $\Delta_f = 0$, where $c^N_{\text{eff}} = 0$). For all other quench protocols, $c^N_{\text{eff}} = 0$. This confirms that the long-range correlations associated with a nonzero effective central charge for both $\alpha = 0$ and $\alpha = 2$ in the stationary state are strictly quantum in nature. On the other hand, for $\alpha = 1$, long-range correlations develop, irrespective of Δ quenches in the critical-to-critical quench protocol (see middle row, left column of Fig. 4). Interestingly, for this quench protocol, c^N_{eff} is slightly larger than c^I_{eff}. In contrast, for the critical-to-noncritical quench protocol, the presence of long-range correlations in the stationary state depends on the Δ quenches. Specifically, if $\Delta_f \Delta_i \gtrsim 0$, both c^I_{eff} and c^N_{eff} are nonzero, whereas both are zero if $\Delta \Delta_0 \lesssim 0$. For all the quench protocols where $\Delta_f \Delta_i \gtrsim 0$, $c^N_{\text{eff}} > c^I_{\text{eff}}$.

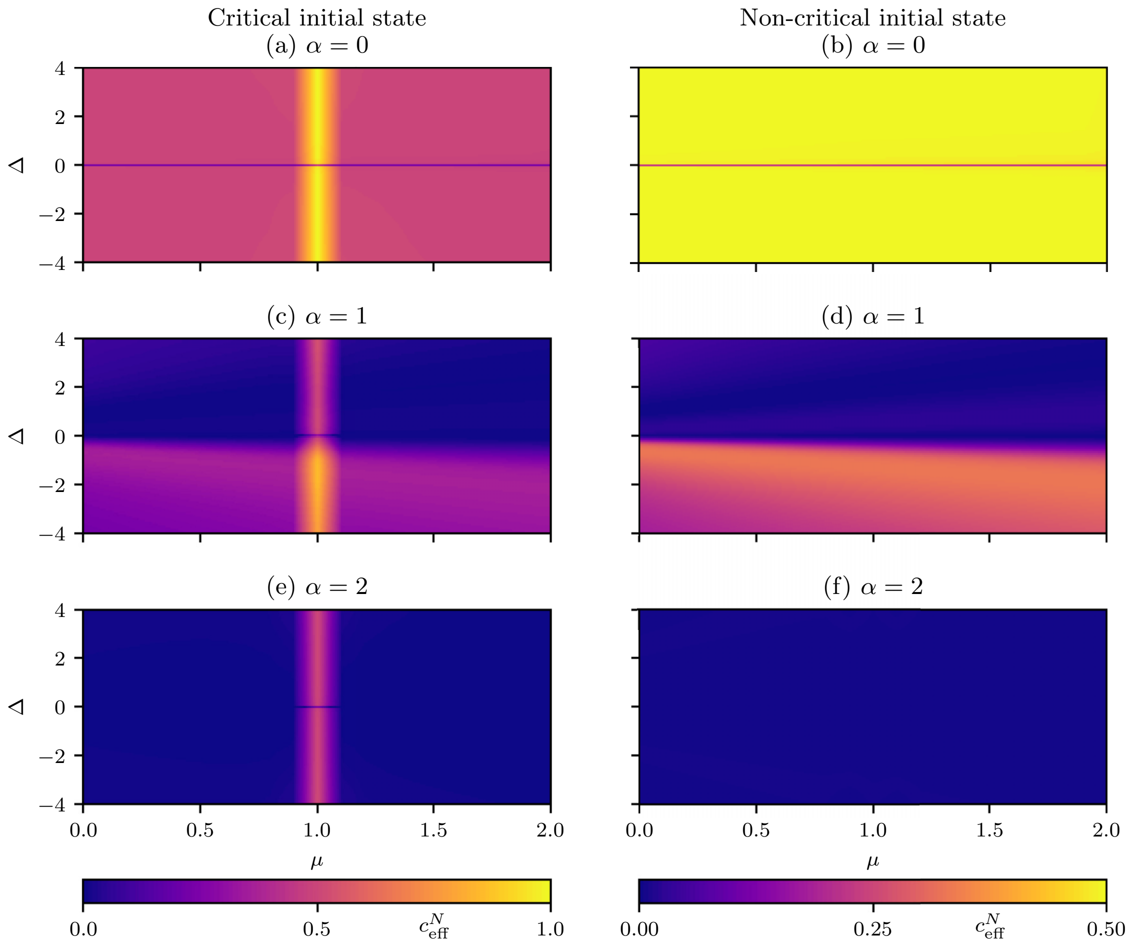

FIG. 4. Phase plot of the effective central charge from log-negativity $c_{\rm eff}^N$ for both critical (left column) and noncritical (right column) initial state for $\alpha = 0$ (top row), 1 (middle row) and 2 (bottom row). The quench parameters are the same as for Fig. 3.

[1] S. Sachdev, *Quantum Phase Transitions*, 2nd ed. (Cambridge University Press, Cambridge, 2011).
[2] T. J. Osborne and M. A. Nielsen, Entanglement in a simple quantum phase transition, Phys. Rev. A **66**, 032110 (2002).
[3] X. Peng, J. Du, and D. Suter, Quantum phase transition of ground-state entanglement in a Heisenberg spin chain simulated in an NMR quantum computer, Phys. Rev. A **71**, 012307 (2005).
[4] R. Dillenschneider, Quantum discord and quantum phase transition in spin chains, Phys. Rev. B **78**, 224413 (2008).
[5] M. Kargarian, R. Jafari, and A. Langari, Renormalization of entanglement in the anisotropic Heisenberg (XXZ) model, Phys. Rev. A **77**, 032346 (2008).
[6] J. Maziero, H. C. Guzman, L. C. Céleri, M. S. Sarandy, and R. M. Serra, Quantum and classical thermal correlations in the XY spin-$\frac{1}{2}$ chain, Phys. Rev. A **82**, 012106 (2010).
[7] F.-W. Ma, S.-X. Liu, and X.-M. Kong, Quantum entanglement and quantum phase transition in the XY model with staggered Dzyaloshinskii-Moriya interaction, Phys. Rev. A **84**, 042302 (2011).
[8] Y.-C. Li and H.-Q. Lin, Thermal quantum and classical correlations and entanglement in the XY spin model with three-spin interaction, Phys. Rev. A **83**, 052323 (2011).
[9] M. M. Rams, M. Zwolak, and B. Damski, A quantum phase transition in a quantum external field: Superposing two magnetic phases, Sci. Rep. **2**, 655 (2012).
[10] Y. Yao, H.-W. Li, C.-M. Zhang, Z.-Q. Yin, W. Chen, G.-C. Guo, and Z.-F. Han, Performance of various correlation measures in quantum phase transitions using the quantum renormalization-group method, Phys. Rev. A **86**, 042102 (2012).
[11] W. W. Cheng, C. J. Shan, Y. B. Sheng, L. Y. Gong, S. M. Zhao, and B. Y. Zheng, Geometric discord approach to quantum phase transition in the anisotropy XY spin model, Physica E **44**, 1320 (2012).
[12] N. Blanc, J. Trinh, L. Dong, X. Bai, A. A. Aczel, M. Mourigal, L. Balents, T. Siegrist, and A. P. Ramirez, Quantum criticality among entangled spin chains, Nat. Phys. **14**, 273 (2018).

[13] D. Jaksch, C. Bruder, J. I. Cirac, C. W. Gardiner, and P. Zoller, Cold bosonic atoms in optical lattices, Phys. Rev. Lett. **81**, 3108 (1998).

[14] M. Greiner, O. Mandel, T. Esslinger, T. W. Hänsch, and I. Bloch, Quantum phase transition from a superfluid to a Mott insulator in a gas of ultracold atoms, Nature (London) **415**, 39 (2002).

[15] B. Capogrosso-Sansone, N. V. Prokof'ev, and B. V. Svistunov, Phase diagram and thermodynamics of the three-dimensional Bose-Hubbard model, Phys. Rev. B **75**, 134302 (2007).

[16] T. Donner, S. Ritter, T. Bourdel, A. Öttl, M. Köhl, and T. Esslinger, Critical behavior of a trapped interacting Bose gas, Science **315**, 1556 (2007).

[17] I. B. Spielman, W. D. Phillips, and J. V. Porto, Mott-insulator transition in a two-dimensional atomic Bose gas, Phys. Rev. Lett. **98**, 080404 (2007).

[18] Z.-W. Zhou, S.-L. Zhang, X.-F. Zhou, G.-C. Guo, X. Zhou, and H. Pu, Quantum phase transition of Bose-Einstein condensates on a nonlinear ring lattice, Phys. Rev. A **83**, 043626 (2011).

[19] D. Rubeni, A. Foerster, E. Mattei, and I. Roditi, Quantum phase transitions in Bose-Einstein condensates from a Bethe ansatz perspective, Nucl. Phys. B **856**, 698 (2012).

[20] J.-Y. Zhang, S.-C. Ji, Z. Chen, L. Zhang, Z.-D. Du, B. Yan, G.-S. Pan, B. Zhao, Y.-J. Deng, H. Zhai, S. Chen, and J.-W. Pan, Collective dipole oscillations of a spin-orbit coupled Bose-Einstein condensate, Phys. Rev. Lett. **109**, 115301 (2012).

[21] Q. Si, S. Rabello, K. Ingersent, and J. L. Smith, Locally critical quantum phase transitions in strongly correlated metals, Nature (London) **413**, 804 (2001).

[22] M. Vojta, Quantum phase transitions, Rep. Prog. Phys. **66**, 2069 (2003).

[23] F. Alet, A. M. Walczak, and M. P. A. Fisher, Exotic quantum phases and phase transitions in correlated matter, Physica A **369**, 122 (2006).

[24] C.-H. Chern, Pseudogap formation and quantum phase transition in strongly-correlated electron systems, Ann. Phys. **350**, 159 (2014).

[25] S. Paschen and Q. Si, Quantum phases driven by strong correlations, Nat. Rev. Phys. **3**, 9 (2021).

[26] H. E. Stanley, Scaling, universality, and renormalization: Three pillars of modern critical phenomena, Rev. Mod. Phys. **71**, S358 (1999).

[27] J. Cardy, *Scaling and Renormalization in Statistical Physics*, Cambridge Lecture Notes in Physics (Cambridge University Press, Cambridge, 1996).

[28] L. P. Kadanoff, Critical behavior, universality and scaling, in *Proceedings of the 1970 Varenna Summer School on Critical Phenomena*, edited by M. S. Green (Academic Press, New York, 1971), pp. 1, 11.

[29] A. Pelissetto and E. Vicari, Critical phenomena and renormalization-group theory, Phys. Rep. **368**, 549 (2002).

[30] A. A. Belavin, A. M. Polyakov, and A. B. Zamolodchikov, Infinite conformal symmetry in two-dimensional quantum field theory, Nucl. Phys. B **241**, 333 (1984).

[31] I. Affleck, Universal term in the free energy at a critical point and the conformal anomaly, Phys. Rev. Lett. **56**, 746 (1986).

[32] P. Di Francesco, P. Mathieu, and D. Sénéchal, *Conformal Field Theory*, Graduate Texts in Contemporary Physics (Springer, New York, 1997).

[33] H. W. J. Blöte, J. L. Cardy, and M. P. Nightingale, Conformal invariance, the central charge, and universal finite-size amplitudes at criticality, Phys. Rev. Lett. **56**, 742 (1986).

[34] P. Ginsparg, Applied conformal field theory, arXiv:hep-th/9108028.

[35] H. E. Stanley, S. V. Buldyrev, A. L. Goldberger, S. Havlin, C.-K. Peng, and M. Simons, Long-range power-law correlations in condensed matter physics and biophysics, Physica A **200**, 4 (1993).

[36] M. B. Hastings and T. Koma, Spectral gap and exponential decay of correlations, Commun. Math. Phys. **265**, 781 (2006).

[37] F. G. S. L. Brandão and M. Horodecki, An area law for entanglement from exponential decay of correlations, Nat. Phys. **9**, 721 (2013).

[38] F. G. S. L. Brandao and M. Horodecki, Exponential decay of correlations implies area law, Commun. Math. Phys. **333**, 761 (2015).

[39] V. Eisler and Z. Zimborás, Area-law violation for the mutual information in a nonequilibrium steady state, Phys. Rev. A **89**, 032321 (2014).

[40] S. Paul, P. Titum, and M. Maghrebi, Hidden quantum criticality and entanglement in quench dynamics, Phys. Rev. Res. **6**, L032003 (2024).

[41] T. Koffel, M. Lewenstein, and L. Tagliacozzo, Entanglement entropy for the long-range Ising chain in a transverse field, Phys. Rev. Lett. **109**, 267203 (2012).

[42] D. Vodola, L. Lepori, E. Ercolessi, and G. Pupillo, Long-range Ising and Kitaev models: Phases, correlations and edge modes, New J. Phys. **18**, 015001 (2015).

[43] J. Eisert, M. Cramer, and M. B. Plenio, *Colloquium:* Area laws for the entanglement entropy, Rev. Mod. Phys. **82**, 277 (2010).

[44] D. Vodola, L. Lepori, E. Ercolessi, A. V. Gorshkov, and G. Pupillo, Kitaev chains with long-range pairing, Phys. Rev. Lett. **113**, 156402 (2014).

[45] M. Saffman, T. G. Walker, and K. Mølmer, Quantum information with Rydberg atoms, Rev. Mod. Phys. **82**, 2313 (2010).

[46] T. Lahaye, C. Menotti, L. Santos, M. Lewenstein, and T. Pfau, The physics of dipolar bosonic quantum gases, Rep. Prog. Phys. **72**, 126401 (2009).

[47] O. Firstenberg, T. Peyronel, Q.-Y. Liang, A. V. Gorshkov, M. D. Lukin, and V. Vuletić, Attractive photons in a quantum nonlinear medium, Nature (London) **502**, 71 (2013).

[48] H. Ritsch, P. Domokos, F. Brennecke, and T. Esslinger, Cold atoms in cavity-generated dynamical optical potentials, Rev. Mod. Phys. **85**, 553 (2013).

[49] B. Yan, S. A. Moses, B. Gadway, J. P. Covey, K. R. A. Hazzard, A. M. Rey, D. S. Jin, and J. Ye, Observation of dipolar spin-exchange interactions with lattice-confined polar molecules, Nature (London) **501**, 521 (2013).

[50] P. Schauß, M. Cheneau, M. Endres, T. Fukuhara, S. Hild, A. Omran, T. Pohl, C. Gross, S. Kuhr, and I. Bloch, Observation of spatially ordered structures in a two-dimensional Rydberg gas, Nature (London) **491**, 87 (2012).

[51] M. Lu, N. Q. Burdick, and B. L. Lev, Quantum degenerate dipolar Fermi gas, Phys. Rev. Lett. **108**, 215301 (2012).

[52] S. Gopalakrishnan, B. L. Lev, and P. M. Goldbart, Frustration and glassiness in spin models with cavity-mediated interactions, Phys. Rev. Lett. **107**, 277201 (2011).

[53] K. Kim, M.-S. Chang, R. Islam, S. Korenblit, L.-M. Duan, and C. Monroe, Entanglement and tunable spin-spin couplings between trapped ions using multiple transverse modes, Phys. Rev. Lett. **103**, 120502 (2009).

[54] J. W. Britton, B. C. Sawyer, A. C. Keith, C.-C. J. Wang, J. K. Freericks, H. Uys, M. J. Biercuk, and J. J. Bollinger, Engineered two-dimensional Ising interactions in a trapped-ion quantum simulator with hundreds of spins, Nature (London) **484**, 489 (2012).

[55] C. Schneider, D. Porras, and T. Schaetz, Experimental quantum simulations of many-body physics with trapped ions, Rep. Prog. Phys. **75**, 024401 (2012).

[56] R. Islam, C. Senko, W. C. Campbell, S. Korenblit, J. Smith, A. Lee, E. E. Edwards, C.-C. J. Wang, J. K. Freericks, and C. Monroe, Emergence and frustration of magnetism with variable-range interactions in a quantum simulator, Science **340**, 583 (2013).

[57] P. Richerme, Z.-X. Gong, A. Lee, C. Senko, J. Smith, M. Foss-Feig, S. Michalakis, A. V. Gorshkov, and C. Monroe, Non-local propagation of correlations in quantum systems with long-range interactions, Nature (London) **511**, 198 (2014).

[58] P. Jurcevic, B. P. Lanyon, P. Hauke, C. Hempel, P. Zoller, R. Blatt, and C. F. Roos, Quasiparticle engineering and entanglement propagation in a quantum many-body system, Nature (London) **511**, 202 (2014).

[59] J. S. Douglas, H. Habibian, C.-L. Hung, A. V. Gorshkov, H. J. Kimble, and D. E. Chang, Quantum many-body models with cold atoms coupled to photonic crystals, Nat. Photon. **9**, 326 (2015).

[60] R. Landig, F. Brennecke, R. Mottl, T. Donner, and T. Esslinger, Measuring the dynamic structure factor of a quantum gas undergoing a structural phase transition, Nat. Commun. **6**, 7046 (2015).

[61] R. Landig, L. Hruby, N. Dogra, M. Landini, R. Mottl, T. Donner, and T. Esslinger, Quantum phases from competing short- and long-range interactions in an optical lattice, Nature (London) **532**, 476 (2016).

[62] A. Bermudez, T. Schaetz, and M. B. Plenio, Dissipation-assisted quantum information processing with trapped ions, Phys. Rev. Lett. **110**, 110502 (2013).

[63] T. Sowiński, One-dimensional Bose-Hubbard model with pure three-body interactions, Open Phys. **12**, 473 (2014).

[64] F. Ares, J. G. Esteve, F. Falceto, and A. R. de Queiroz, Entanglement in fermionic chains with finite-range coupling and broken symmetries, Phys. Rev. A **92**, 042334 (2015).

[65] C. Holzhey, F. Larsen, and F. Wilczek, Geometric and renormalized entropy in conformal field theory, Nucl. Phys. B **424**, 443 (1994).

[66] G. Vidal, J. I. Latorre, E. Rico, and A. Kitaev, Entanglement in quantum critical phenomena, Phys. Rev. Lett. **90**, 227902 (2003).

[67] P. Calabrese and J. Cardy, Entanglement entropy and quantum field theory, J. Stat. Mech. (2004) P06002.

[68] P. Calabrese and J. Cardy, Entanglement entropy and conformal field theory, J. Phys. A: Math. Theor. **42**, 504005 (2009).

[69] M. A. Cazalilla, R. Citro, T. Giamarchi, E. Orignac, and M. Rigol, One dimensional bosons: From condensed matter systems to ultracold gases, Rev. Mod. Phys. **83**, 1405 (2011).

[70] R. Dorner, J. Goold, C. Cormick, M. Paternostro, and V. Vedral, Emergent thermodynamics in a quenched quantum many-body system, Phys. Rev. Lett. **109**, 160601 (2012).

[71] L. Lepori, S. Paganelli, F. Franchini, and A. Trombettoni, Mutual information for fermionic systems, Phys. Rev. Res. **4**, 033212 (2022).

[72] B. Groisman, S. Popescu, and A. Winter, Quantum, classical, and total amount of correlations in a quantum state, Phys. Rev. A **72**, 032317 (2005).

[73] Y.-W. Dai, X.-H. Chen, S. Y. Cho, and H.-Q. Zhou, Critical exponents of block-block mutual information in one-dimensional infinite lattice systems, Phys. Rev. E **104**, 044137 (2021).

[74] J.-M. Stéphan, Shannon and Rényi mutual information in quantum critical spin chains, Phys. Rev. B **90**, 045424 (2014).

[75] F. C. Alcaraz and M. A. Rajabpour, Universal behavior of the Shannon and Rényi mutual information of quantum critical chains, Phys. Rev. B **90**, 075132 (2014).

[76] J. Wilms, J. Vidal, F. Verstraete, and S. Dusuel, Finite-temperature mutual information in a simple phase transition, J. Stat. Mech. (2012) P01023.

[77] M. B. Plenio, Logarithmic negativity: A full entanglement monotone that is not convex, Phys. Rev. Lett. **95**, 090503 (2005).

[78] G. Vidal and R. F. Werner, Computable measure of entanglement, Phys. Rev. A **65**, 032314 (2002).

[79] J. Eisert and M. B. Plenio, A comparison of entanglement measures, J. Mod. Opt. **46**, 145 (1999).

[80] M. Horodecki, P. Horodecki, and R. Horodecki, Separability of mixed states: Necessary and sufficient conditions, Phys. Lett. A **223**, 1 (1996).

[81] P. Calabrese, F. H. L. Essler, and M. Fagotti, Quantum quench in the transverse field Ising chain: I. Time evolution of order parameter correlators, J. Stat. Mech. (2012) P07016.

[82] I. Peschel, Calculation of reduced density matrices from correlation functions, J. Phys. A: Math. Gen. **36**, L205 (2003).

[83] K. Sengupta, S. Powell, and S. Sachdev, Quench dynamics across quantum critical points, Phys. Rev. A **69**, 053616 (2004).

[84] V. Eisler and Z. Zimborás, On the partial transpose of fermionic Gaussian states, New J. Phys. **17**, 053048 (2015).

[85] A. Coser, E. Tonni, and P. Calabrese, Partial transpose of two disjoint blocks in *XY* spin chains, J. Stat. Mech. (2015) P08005.

[86] H. Shapourian, K. Shiozaki, and S. Ryu, Partial time-reversal transformation and entanglement negativity in fermionic systems, Phys. Rev. B **95**, 165101 (2017).

[87] J. Eisert, V. Eisler, and Z. Zimborás, Entanglement negativity bounds for fermionic Gaussian states, Phys. Rev. B **97**, 165123 (2018).

[88] G. Roósz, Z. Zimborás, and R. Juhász, Entanglement scaling in fermion chains with a localization-delocalization transition and inhomogeneous modulations, Phys. Rev. B **102**, 064204 (2020).

[89] C. P. Herzog and Y. Wang, Estimation for entanglement negativity of free fermions, J. Stat. Mech. (2016) 073102.

[90] M. Rota, Tripartite information of highly entangled states, J. High Energy Phys. 04 (2016) 075.

[91] P. Hosur, X.-L. Qi, D. A. Roberts, and B. Yoshida, Chaos in quantum channels, J. High Energy Phys. 02 (2016) 004.

[92] F. Caceffo and V. Alba, Negative tripartite mutual information after quantum quenches in integrable systems, Phys. Rev. B **108**, 134434 (2023).

[93] N. J. Cerf and C. Adami, Information theory of quantum entanglement and measurement, Physica D **120**, 62 (1998).

[94] V. Marić and M. Fagotti, Universality in the tripartite information after global quenches, Phys. Rev. B **108**, L161116 (2023).

[95] R. Rattazzi, S. Rychkov, and A. Vichi, Central charge bounds in 4D conformal field theory, Phys. Rev. D **83**, 046011 (2011).

[96] G. Delfino, Particles, conformal invariance and criticality in pure and disordered systems, Eur. Phys. J. B **94**, 65 (2021).

[97] Note that $\Delta = 0$ completely changes the Hamiltonian to a nearest-neighbor model with no pairing term with effective central charge 0 for $\mu \neq 1$.